Influence of bond interface over the lap-shear performance of 3D printed multi-material samples.

Vasile Ermolai[1*,2[0000-0001-5967-5748]] Alexandru Sover [2[0000-0003-3408-898X]] and Gheorghe Nagîț[1[0000-0001-9649-8525]]

1 "Gheorghe Asachi" Technical University of Iasi, Department of Machine Manufacturing Technology, Blvd. Dimitrie Mangeron 59A, Iasi, 700050, Romania
2 Ansbach University of Applied Science, Faculty of Technology, Residenzstraße 8, Ansbach, 91522, Germany
*vasile.ermolai@hs-ansbach.de

Abstract. Multi-material 3D printing offers new possibilities regarding product development, allowing design freedom and multiple materials choices in terms of colour and polymer type. Material extrusion technologies are among the most popular options for multi-material printing due to their low equipment cost and various thermoplastic materials. However, polymers' compatibility and bond interface must be considered for multi-material components. Material Extrusion creates the parts layer by layer, and each layer is characterised by multiple lines of extruded thermoplastic at a defined width. Therefore, regardless of the 3D model's surfaces, they are composed of numerous lines of material and voids. Depending on the 3D Printing process setup, the bonding mechanism between materials can be influenced due to the different characteristics of horizontal and vertical contact interfaces. For this reason, this paper aims to study the influence of process parameters over horizontal interface through lap-shear tests for multi-materials samples made of acrylonitrile butadiene styrene (ABS), acrylonitrile styrene acrylate (ASA), and polycarbonate (PC). The results show that bond interface strength can be improved by creating ways for the mechanical interlock of the materials.

Keywords: Fused Filament Fabrication, Multi-material, Bond interface, Process parameters, Lap shear.

1 Introduction

Additive manufacturing (AM) technologies allow more design freedom and possibilities for designing functional parts. A part of the design freedom is given by the materials composition of the final product. AM technologies such as Fused Filament Fabrication – FFF can produce multi-materials components in a single process [1]. FFF proved that it is suitable for manufacturing functional parts, sandwich panels [2], shape-memory structures [1, 3, 4], medical applications [1], and others.

Multi-material FFF introduced new possibilities regarding the part complexity, combination of different materials blends and product customisation [1,5]. However, multi-material parts can be manufactured only if specific requirements regarding the materials (e.g., compatibility), geometry, process parameters (e.g., deposition speed), and environmental conditions (e.g., printing in an enclosure) are respected [6, 7].

Regardless of materials, the strength of multi-material parts is based on the materials' contact interface between mating bodies. It is more frequently known as a bond, contact interface or just interface [9]. Depending on the materials' chemical affinity, the multi-material parts can be made of similar or dissimilar materials.

Some studies evaluated the strength of the contact interface from the geometrical perspective using macroscopic joints (e.g., T-shape, Dovetail). This way, it was possible to obtain strong samples of dissimilar materials [9].

On the other hand, for chemically compatible materials, the strength of the interface is given by the adhesion mechanism between materials. This way, the materials' bond can be obtained through diffusion, adsorption, mechanical interlocking, and others. The bonding mechanisms are comprised of the adhesion theory. Even if the adhesion mechanisms are described independently of the materials' bond formation, they take place simultaneously and are hard to quantify independently [5]. For these materials, multiple studies are available in the literature, describing the adhesion mechanism of horizontal interface or interlayer bond [8, 10], vertical interface [11] or both [12, 13].

This study focuses only on horizontal interface parametrisation to understand how the process parameters influence the multi-material parts' adhesion mechanism.

2 Methods

2.1 Bond interface definition

Through FFF, parts are made by adding consecutive layers of a defined thickness (e.g., 0.2 mm). Depending on the layer number, this can be constructed differently. Frequently, the first layer is composed of multiple walls and solid fill, while an intermediary layer from walls and infill. Because layers are deposited on top of the previous, each contact between material layers can be considered an interface. For multi-material FFF, the horizontal interface is situated between the base material's last layer and the second material's bottom layer.

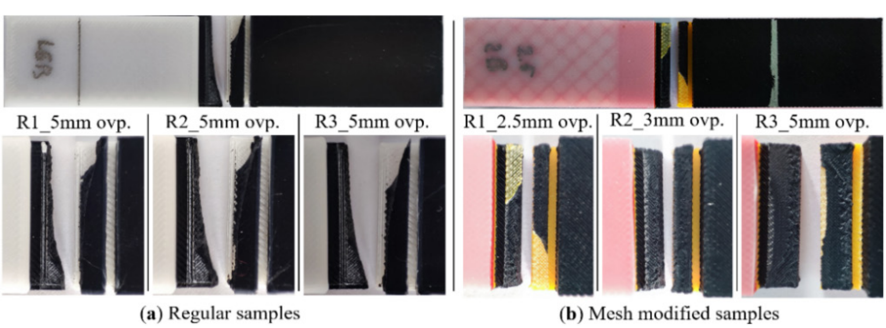

Fig. 1. The failure mode of preliminary lap-shear specimens: (a) Full density samples with 5 mm overlap; (b) Mesh modified samples with 2.5, 3, and 5-mm overlap.

The bond interface strength of multi-material samples was evaluated with lap shear testing. The test model is based on ISO 11003-2:2019(E) sample adapted by Watschke et al. [14] for multi-material AM. Since the proposed specimen was tested only for low-compatibility materials, a set of preliminary trials (i.e., three of each setup) was necessary to determine if the used approach fits compatible materials testing (see Fig. 1).

The preliminary models were printed using ABS and ASA materials with three walls and a solid fill for each layer. Similar failure modes characterised the resulting samples. The specimens failed in the ASA material zone, and crack propagation started at the mating zone between the walls and solid fill (see Fig.1a).

Based on those findings, the second set of specimens was printed without walls and with three overlapping region sizes 5 (i.e., tested by Watschke et al. [14]), 3, and 2.5 mm between the mating bodies. The resulting samples are customised using mesh modifiers to reduce material consumption and printing time. This way, the specimen's structure can be adjusted locally, only where the modifiers overlap the 3D model. Therefore, the samples were printed with a full density in the overlapping region (i.e., 10mm from the midplane) and 25% for the remaining (using the M1 mesh modifier from Fig. 2). Again, the samples failed predominantly on the ASA side but with different failure modes among each group (see Fig. 1b). The goal was to identify which of the considered overlaps detach at the interface level. Based on the results, the 2.5 mm overlap was considered optimum for evaluating compatible multi-material samples' horizontal interface strength (see Fig. 1b). Secondly, the considered mesh modifiers are used for the entire study. Their working principle and effects are described in Fig. 2.

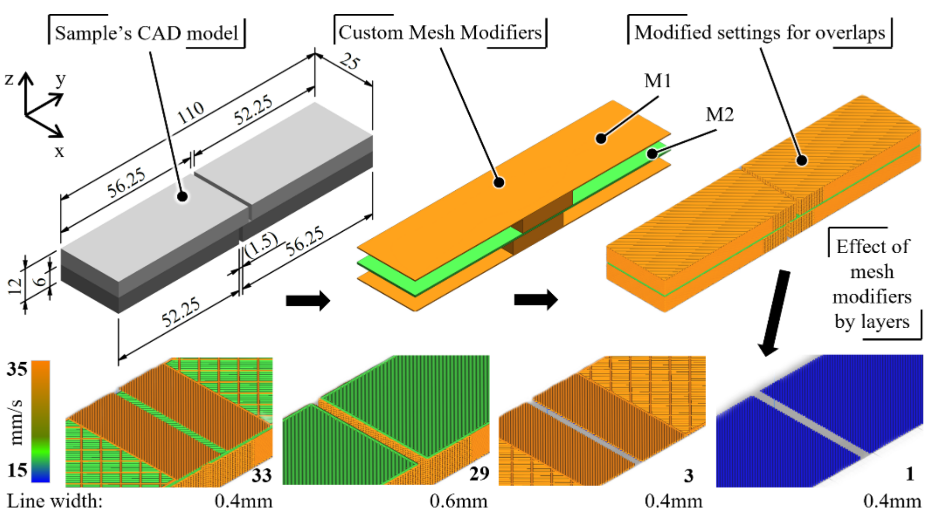

Fig. 2. The effect of using mesh modifiers on the lap-shear samples (R9 configuration).

2.2 Design of the experiment

A Taguchi L9 matrix was considered for this study, with four factors and three-level variations. The chosen factors control only the last two layers of the first material and the first two of the second material via M2 mesh modifiers (see Fig. 2). Their designation and levels are presented in Table 1.

Table 1. Variable parameters of the bond interface with the resulting experimental matrix.

	Factors/Levels	L1	L2	L3
1	Interface Line Width – ILW	0.4	0.5	0.6
2	Interface Line Directions – ILD	0/90	30/120	45/135
3	Interface Line Overlap – ILO	0	12.5	25
4	Interface Print Speed – IPS	20	30	40

Run order/	Taguchi L9 matrix (4^3)			
Factors	ILW	ILD	ILO	IPS
R1	0.4	0/90	0	20
R2	0.4	30/120	12.5	30
R3	0.4	45/135	25	40
R4	0.5	0/90	12.5	40
R5	0.5	30/120	25	20
R6	0.5	45/135	0	30
R7	0.6	0/90	25	30
R8	0.6	30/120	0	40
R9	0.6	45/135	12.5	20

ILW controls the line width of the interface. A smaller line width (i.e., 0.4mm) will generate smaller gaps between the extrusion paths, and a wider line (i.e., 0.6mm) will create larger gaps. Because when printing, the molten material will follow the topography of the interface, this factor will provide information on which solution is better: more gaps with a smaller size or fewer but bigger.

The second parameter, ILD, controls the solid fill's line directions. Line directions are believed to influence gap sizes between lines and load capacity.

ILO regulates the overlap between the extruded lines. This parameter is important for surface quality. If the overlap is insufficient, gaps occur, and if too high, the molten material will be forced out, creating scratches on the top surface.

The last factor, IPS, controls the molten thermoplastic's deposition speed. The printing speed is dependent on the chosen material and extruder capacity to provide a constant flow of molten material. If the extrusion speed is too high inconsistent extrusion may occur, resulting in gaps between the extrusion paths. On the other hand, printing speed plays a significant role in intra-layer and inter-layer fused. The lower the speed, the better the bonding between extruded lines.

As presented above, all considered factors could influence the bond interface's interface quality. The experimental matrix shown in Table 1 will be used to evaluate the lap-shear performance of the compatible material pairs: ABS-PC, ABS-ASA, and ASA-PC. The general print settings are presented in the following subsection.

2.3 Process parametrisation

Three filaments were chosen for this study: a white colour Ultrafuse ABS from BASF, a red ApolloX ASA from FormFutura, and a black PolyMax PC from Polymaker. The 3D models were sliced using Cura 4.13.1 and printed using an Ultimaker 3 in dual extrusion mode with 0.4 mm nozzles. Due to the materials' thermal sensitivity, the samples were printed in a closed environment after the air temperature reached 40°C. The values of the rest of the controlled process parameters are presented in Table 2.

Table 2. The constant parameters used for printing the lap-shear specimens.

1	Layer height (mm)	0.2	9	First layer speed (mm/s)	15
2	Line width (mm)	0.4	10	Retraction speed (mm/s)	30/**35**/*35*
3	Wall line count (no.)	1	11	Retraction distance (mm)	8/**7**/*7*
4	Top/Bottom layers (no.)	0	12	Fan speed (%)	3/**3**/*0*
5	Infill percentage (%)	25	13	Brim line count	4
6	Infill pattern	Grid	14	Merged meshes overlap (mm)	0
7	Material flow (%)	100	15	Bed temperature (°C)	100
8	Print speed (mm/s)	35	16	Extrusion temperature (°C)	250/**255**/*265*

Values in bold are associated with the ASA filament;
Values in italic are associated with the PC filament.

A notable mention is the *Merged Meshes overlap* setting, available in Cura's *Mesh Fixes* tab. According to the slicing guide, this setting controls the overlap between mating bodies to improve strength. For this study, its value was set at 0 mm.

3 Results and discussion

The specimens were tested in the same laboratory condition, having 22°C and 47% humidity using an MTS Criterion Model 43 universal testing machine with a load cell of 5 kN. Four samples were tested for each pair of materials. The resulting average maximum force, displacement at break and the samples' failure mode were used to evaluate the bond interfaces.

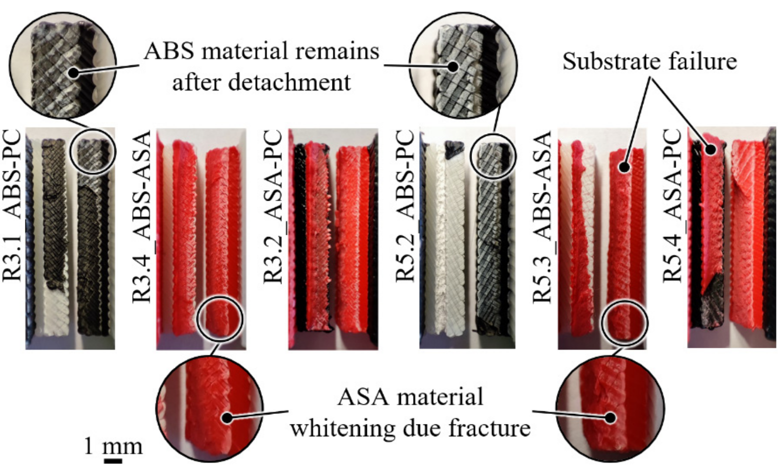

Fig. 3. Example of the failure mode of the R3 and R5 interfaces for each group of materials.

Three failure scenarios were registered for the lap-shear samples, interface detachment, substrate rupture or a combination of them, and the most frequent break patterns were the last two. As presented in Fig. 3, substrate failure was characterised by the partial detachment of the first two layers under the transition interface (e.g., sample R3.1) or by in-depth rupture of the materials under the interface, which is characterised by white marks of crazing (e.g., R3.2, R3.4). For the specimens which showed zones of interface detachment, traces of the mating material can be observed (e.g., R3.1, R5.2 samples for ABS and R5.4 for ASA). Depending on the interface setup, the amount of material remains on the mating bodies differed. For example, in the case of ABS-PC samples, the R5 interface shows a better material fuse than R3 (see Fig. 3). The results can be explained by the different setups of the two interfaces (see Table 1). It is supposed that due to slower printing speed (i.e., 20 mm/s), the R5 interfaces had a better material fuse than the R3 interface. The average results of the maximum force and displacement at break are presented in Fig. 4.

The results show a low variation of the maximum force and displacement at the break. The highest variation was recorded for the ABS-PC R1 configuration with a standard deviation of 0.098 kN. For displacement, the highest deviation was recorded for the same material group in the R3 setup, having 0.162 mm.

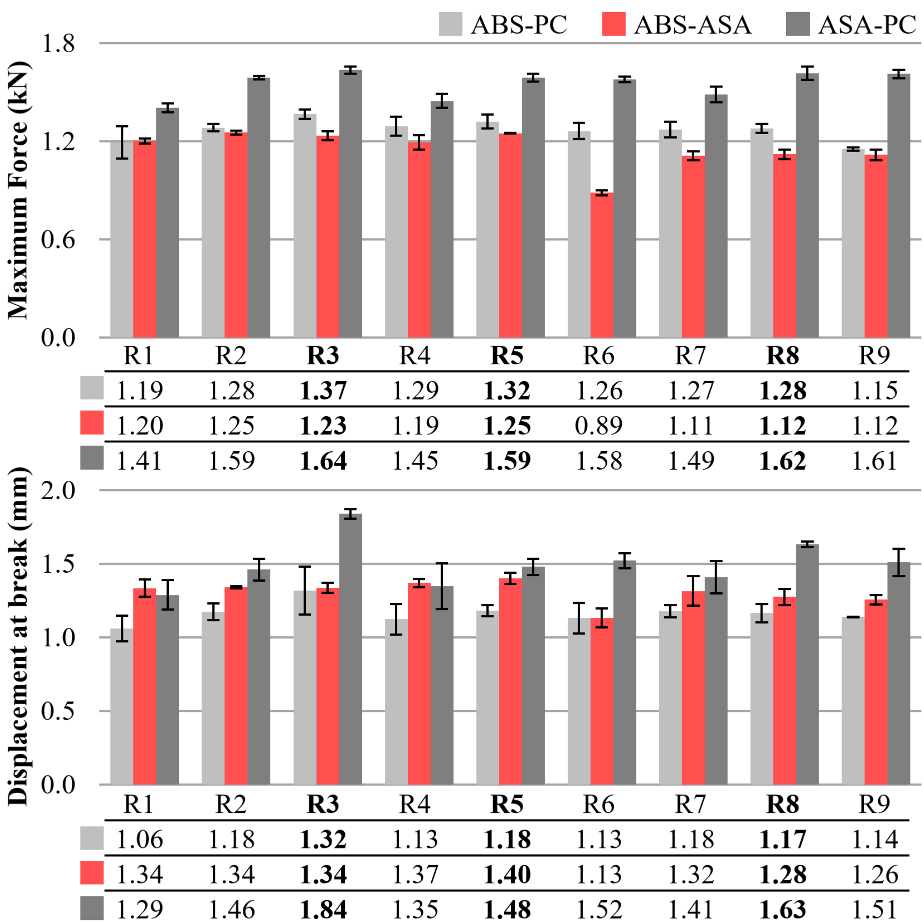

Fig. 4. Average load and displacement for the lap-shear specimens.

Regardless of the samples' materials groups, the best results were obtained by the R3 interface, having an 0.4 mm line, a 25% overlap and a 45°/135° lines direction and printed at 40 mm/s. However, comparable results were obtained for wider extrusion lines for the R5 and R8 interfaces (see Fig. 4).

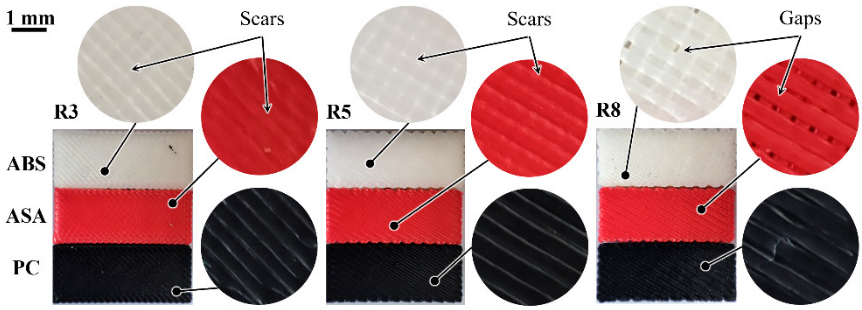

Fig. 5. Detailed view of the interface for R3, R5 and R8 configurations.

Because the R3 interfaces were printed with a 25% overlap of the lines, the resulting surfaces presented material excess at the level of the weld line. This way, the extra amount of material was forced out, creating scars on the top surface (an over-extrusion). Those scars gave way to a mechanical interlock with the top material (see Fig. 5).

For R5 and R8 interfaces, the best results were obtained for the 30°/120° line orientation but with different levels for the other factors. The R5 interface was printed at 20 mm/s with 25% overlap between lines, and the R8 at 40 mm/s with no overlap.

In the case of the R5 interface, due to the increased width and overlap of the lines, the excess material created scars on the top surface, showing the same bond pattern as the R3 setup. On the other hand, for the R8 interface, because of the wide line of 0.6 mm, no overlap between the lines and a relatively high extrusion speed of 40 mm/s, the extruder was incapable of feeding enough material creating gaps between the lines (an under-extrusion). The resulting gaps offered a way of mechanical interlock for the mating material. The resulting interfaces of the R3, R5 and R8 printing configurations are presented above in Fig. 5.

Table 3. Size of the main effects based on the responses and the resulting ranks of the factors.

Material	Effect's size	Means of Forces (kN)				Effect's size	Means of Displacements (mm)			
		ILW	ILD	ILO	IPS		ILW	ILD	ILO	IPS
ABS-PC	Delta	0.058	0.042	0.076	0.091	Delta	0.038	0.075	0.107	0.075
	Rank	3	4	2	**1**	Rank	4	3	**1**	2
ABS-ASA	Delta	0.120	0.129	0.128	0.107	Delta	0.056	0.098	0.104	0.067
	Rank	3	**1**	2	4	Rank	4	2	**1**	3
ASA-PC	Delta	0.33	0.163	0.036	0.031	Delta	0.080	0.274	0.136	0.181
	Rank	3	**1**	2	4	Rank	4	**1**	3	2

The resulting averages for maximum force and displacement (see Fig. 4) were used as a response for the Taguchi L9 experimental matrix. Using Minitab, each variable's rank was determined along with the factorial plots. As can be observed in Table 3, The importance of the considered factor differs between the material pairs. The most significant factor for maximum force for the ABS-PC pair is IPS, followed by ILO, ILW, and ILD. The other two materials groups have a different ranking, where ILD is the most significant variable, followed by ILO, ILW and IPS. The average displacement results show that for ABS-PC and ABS-ASA, the most significant influence is given by the ILO and for ASA-PC by ILD.

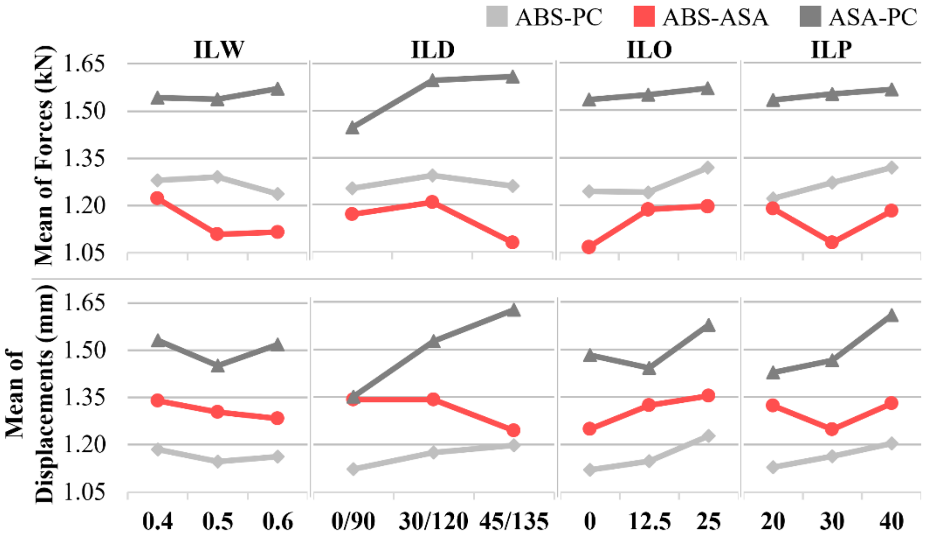

Fig. 6. Main effect plots of maximum force and displacement for each materials pair.

By analysing the main effects plots (see Fig. 6), it can be observed that the influence of each factor level differs for the evaluated responses and materials, ILW and ILD showing the highest variation of the effects. Thus, it is hard to appreciate which factor level influences the interface most. However, for ILO and IPS, for both analysed responses, the maximum effect can be obtained by using a 25% line overlap and 40 mm/s printing speed. As observed previously, those settings created gaps and scars on the interface surface, which provided a mechanical interlocking way for the mating material. By correlating these two analyses, it can contend that the lap-sear performance can increase by creating asperities and voids (i.e., defects) at the bond interface level by printing settings.

4 Conclusions

Multimaterial FFF shows great potential for producing engineering-grade components. The adhesion theory describes multiple bond formation mechanisms, but it is challenging to describe them independently.

This research investigated the influence of line width, orientation and overlap at different print speeds over the horizontal bond interface of three compatible thermoplastic materials. The resulting interfaces were evaluated through lap-shear testing. The results show that the considered factors' different effects depend on the materials combination or the analysed response.

By correlating the print results of the interfaces and the main variables, it was concluded that defects on the base interface, such as scratches and gaps, create ways for the mating materials to interlock mechanically. Further research needs to be done to describe the bond mechanism of multi-material components.

References

1. Singh, S., Singh, G., Prakash, C., Ramakrishna, S., Current status and future directions of fused filament fabrication. J. Manuf. Process. 55, 288-306 (2020).
2. Prajapati, M., J., Kumar, A., Lin, S.C., Jeng, J.Y., Multi-material additive manufacturing with lightweight closed-cell foam-filled lattice structures for enhanced mechanical and functional properties. Addit. Manuf. 54, 102766 (2022).
3. Chu, H., Yang, W., Sun, L., Cai, S., Yang, R., Liang, W., Yu, H., Liu, L., 4D Printing: A Review on Recent Progresses. Micromachines 11(9), 796 (2020).
4. Peng B., Yang, Y., Ju, T., Cavicchi, K.A., Fused Filament Fabrication 4D Printing of a Highly Extensible, Self-Healing, Shape Memory Elastomer Based on Thermoplastic Polymer Blends. ACS Appl. Mater. Interfaces 13, 12777-12788 (2021).
5. Freund, R., Watschke, H., Heubach, J., Vietor, T., Determination of Influencing Factors on Interface Strength of Additively Manufactured Multi-Material Parts by Material Extrusion. Appl. Sci. 9, 1782 (2019).
6. Popescu, D., Zapciu, A., Amza, C., Baciu, F., Marinescu, R., FDM process parameters influence over the mechanical properties of polymer specimens: A review. Polymer Testing 69, 157-166 (2018).
7. Zhou, M., Zhou, X., Si, L., Chen, P., Li, M., Zhang, Y., Zhou, H., Modeling of bonding strength for Fused Filament Fabrication considering bonding interface evolution and molecular diffusion, J. Manuf. Process. 68, 1485-1494 (2021).
8. Gao, X., Qi, S., Kuang, X., Su, Y., Li, J., Wang, D., Fused filament fabrication of polymer materials: A review of interlayer bond. Addit. Mnuf. 37, 101658 (2021).
9. Ribeiro, M., Carneiro, O.S., Interface geometries in 3D multi-material prints by fused filament fabrication. Rapid Prototyp. J. 25(1), 38-46 (2019).
10. Harris, C.G., Jursik, N.J.S., Rochefort, W.E., Walker, T.W., Additive Manufacturing with soft TPU-Adhesion strength in multimaterial flexible joints. Front. Mech. Eng. 5, 37 (2019).
11. Hasanov S., Gupta, A., Nasirov, A., Fidan, O., Mechanical characterisation of functionally graded materials produced by the fused filament fabrication process. J. Manuf. Process. 58, 923-935 (2020).
12. Ando, M., Birosz, M., Jeganmohan, S., Surface bonding of additive manufactured parts from multi-colored PLA materials. Measurement 169, 108583 (2021).
13. Ermolai, V., Sover, A., Nagîț, G.: Influence of contact geometry over the filament bond of polylactic acid blends. In: Conf. Ser.: Mater. Sci. Eng., vol. 1235, 012004, (2021).
14. Watschke, H., Waalkes, L., Schumacher, C., Vietor, T., Development of Novel Test Specimens for Characterisation of Multi-Material Parts Manufactured by Material Extrusion. Appl. Sci. 8, 1220 (2018).